16th World Conference on Earthquake, 16WCEE 2017

Santiago Chile, January 9th to 13th 2017

Paper N° 1248

Registration Code: S-Y1461928394

ACCELERATION TRACKING CONTROL FOR UNIAXIAL SHAKING TABLES CONSIDERING SYSTEM PERFORMANCE AND ROBUSTNESS

P. C. Chen [(1)], C. T. Lai [(2)]

[(1)] *Associate Researcher, National Center for Research on Earthquake Engineering, Taipei, Taiwan, pcchen@ncree.narl.org.tw*

[(2)] *Graduate Student, Department of Civil Engineering, National Taiwan University, Taipei, Taiwan, r03521207@ntu.edu.tw*

Abstract

Shaking table testing has been regarded as one of the most direct experimental methods to evaluate the seismic response of structural systems subjected to earthquake ground motions. A typical uniaxial shaking table is composed of a hydraulic actuator, a servo valve, a digital controller, and a rigid platen. By driving the actuator, the seismic response of the structure mounted on the rigid platen can be investigated. However, it is difficult to reproduce earthquake acceleration accurately by using the commercial proportional-integral-derivative controller in displacement control mode. Therefore, acceleration control becomes essential to improve the performance of the shaking table. In this paper, an acceleration tracking control method for uni-axial shaking tables is proposed. System dynamics which considers the control-structure interaction is first identified. Then the analyses and syntheses of the feedforward and feedback controllers can be conducted. The feedforward controller is to shape the frequency response of the desired acceleration to improve the tracking performance of the shaking table test system. Inverse model technique is used to design the feedforward controller. On the other hand, the feedback controller is to enhance the stability margin considering the system uncertainty. Loop-shaping method is adopted to design the feedback controller. This control framework is realized by using advanced hardware and software, allowing rapid outer-loop controller implementation. Finally, experimental validation is carried out to investigate the control performance. Experimental results indicate that the feedforward controller can effectively increase the frequency bandwidth of the table acceleration while the feedback controller further strengthens the system robustness.

Keywords: acceleration tracking, shaking table, system performance, system robustness

1. Introduction

Shaking table testing provides a direct process to assess dynamic responses of civil engineering structures under earthquake excitation. Traditionally, the hydraulic actuators used in shaking tables are displacement-controlled by employing proportional-integral-differential (PID) control algorithms where reference displacements are determined a priori by double integrating the desired acceleration time history and removing drifting components through baseline correction methods. In a PID control loop, the magnitude, integral, and derivative of the difference between the desired and measured displacements are multiplied by three predefined values, namely proportional, integral, and derivative gains. The control signals to the shaking table are manipulated by the summation of the three individual terms. The PID controller used for displacement control provides reasonable performance in the low frequency range; however, the accuracy of acceleration reproduction is not guaranteed over the frequency of interest. In addition, the three control gains are generally tuned and determined prior to the test which indicates that PID control may not perform well after the nonlinear softening behavior of the specimen occurs.

Several researchers have proposed control methods to improve the control performance of shaking tables. Spencer and Yang [1] proposed the transfer function iteration method which was based on a linearized model of the shaking table from displacement commands to measured accelerations. The command signal time history can be generated from the desired acceleration record by an inverse model. Stoten and Gomez [2] presented the minimal control synthesis algorithm for shaking tables which allows online tuning the controller without any necessary knowledge of system dynamics in advance. Nakata [3] developed a combined control scheme including acceleration feedforward, displacement feedback, command shaping, and a Kalman filter for measured displacements. Phillips et al. [4] proposed a model-based multi-metric control strategy to improve the acceleration tracking of shaking table by using both displacement and acceleration measurements. These aforementioned methods improve control accuracy of shaking table acceleration tracking over a wide range of frequencies; however, control synthesis and applications considering both system robustness and characteristics of ground motions are rare.

In this paper, a shaking table control framework is proposed which considers the tracking performance and system robustness. In addition to a typical inner-loop PID controller which is responsible for the system stability, the proposed control framework is regarded as outer-loop controllers that are implemented around such an inner-loop controller. The objective is to improve the acceleration tracking performance as well as the robustness against the system uncertainty and unmodeled dynamics of the shaking table. This framework consists of a feedforward controller and a feedback controller. The feedforward controller shapes the reference displacement and acceleration to increase the bandwidth of the shaking table. A linear interpolation algorithm which takes the characteristics of the desired acceleration time history is proposed to select the weightings for calculating the control command from the shaped displacement and acceleration. The feedback controller strengthens the system robustness through the loop-shaping method. The proposed framework is verified by using a self-developed uniaxial shake table to investigate its feasibility and effectiveness. Finally, the control performance of the experimental validation is discussed and summarized.

2. Feedforward Controller

The feedforward controller is designed to improve the bandwidth of shaking table test system by cancelling its dynamics. It shapes the frequency response of the desired reference to improve the tracking performance of the system as illustrated in Fig. 1 in which the displacement shaping controller is taken as an example. $G_{xu}(s)$ represents the transfer function between the desired and achieved displacements of the shaking table, and s is a complex number in the Laplace transform. It is noted that a perfect inverse control results in an exact replica of the desired response with unity magnitude and zero phase difference.

The system dynamics of a shaking table is casual which indicates the system outputs barely depend on the current and/or past inputs. In terms of the transfer function of a causal system, the degree of the denominator is greater than or equal to the degree of the numerator. Generally, the transfer function of a uniaxial shaking table can be represented as

$$G_{xu}(s) = \frac{n_m s^m + n_{m-1} s^{m-1} + \ldots + n_0}{d_n s^n + d_{n-1} s^{n-1} + \ldots + d_0} \tag{1}$$

where $d_n, \cdots, d_0$ and $n_m, \cdots, n_0$ are the coefficients in the denominator and the numerator, respectively. If $n \geqq m$, the system is causal. It is noted that a non-causal system is obtained when taking the inverse of a causal system. The outputs of a non-causal system are affected by the future inputs. Therefore, the inverse of an existing shaking table dynamics is non-causal and cannot be directly implemented with a real-time digital machine. Phillips and Spencer [5] used the central difference method with a linear acceleration extrapolation while Asai et al. [6] adopted the backward difference method to implement the inverse system. The results show that the system dynamics can be accurately inversed within a limited frequency bandwidth by using the two methods.

In this paper, the inverse identification method is proposed to resolve the causality quandary by releasing the constraint of zero phase difference. In other words, the magnitude ratio between the input and output of the open loop is remained unity but nonzero phase is allowable. Band-limited white noise (BLWN) is first adopted as the reference input to excite the shaking table and the achieved displacement and acceleration of the shaking table are measured. Then, take the inverse of the input and output, and find the transfer function that matches the experimental data by using least square regressive method. In this study, both the displacement and acceleration feedforward controllers are constructed by using the proposed inverse identification.

Weighting selection method is essential for combining both the displacement and acceleration feedforward controllers. It is known that displacement control in shake tables performs fairly well in the low frequency range; however, it produces poor acceleration tracking in the high frequency range. As a result, a combined displacement and acceleration feedforward controllers are proposed to generate the command for the inner-loop PID control system. Figure 2 shows the block diagram of the proposed weighted feedforward controller implementation where W_x and W_a are the weightings for the displacement and acceleration feedforward controllers, respectively. It is noted that the weightings W_x and W_a must satisfy $W_x + W_a = 1$. $G_{au}(s)$ represents the transfer function between the command and achieved acceleration of the shaking table. The displacement reference $r_x(t)$ can be obtained by converting the acceleration reference to displacement reference through transfer functions online. Consequently, the command u(t) sent to the inner-loop PID control system can be calculated as

$$u(t) = W_x G_{xu}{}^{-1}(s) r_x(t) + W_a G_{au}{}^{-1}(s) r_a(t) \tag{2}$$

The weighting selection depends on the frequency characteristics of the acceleration to be reproduced. Disregarding the control-structure interaction (CSI) [7], the table displacement should be double integral of the table acceleration. Accordingly, there is an s^2 term in the denominator of the transfer function between the displacement command and the achieved acceleration. As the frequency of the displacement command approaches to zero, the achieved acceleration is also close to zero. It indicates the acceleration feedforward controller is not effective for acceleration tracking in the low frequency range. In addition, an accelerometer normally may not be good enough to measure the response in low frequencies even though the lowest frequency response is claimed DC. Consequently, displacement control is preferred in the low frequency range while acceleration control is favored in the high frequency range in this study.

The method for determining the weightings for the displacement and acceleration feedforward controllers is described in the following. First, Fourier transform of the acceleration reference is conducted and the corresponding centroid frequency of the area in the frequency domain can be calculated as

$$f_c = \frac{\sum_{k=1}^{N} F[k] f[k]}{\sum_{k=1}^{N} f[k]} \tag{3}$$

where f_c is the frequency of the centroid; N is the number of frequency points in Fourier transform; $F[k]$ and $f[k]$ are the magnitude and frequency datum in Fourier transform, respectively. Then, plot the Bode diagram of $G_{xu}(s)$ and $s^2G_{au}(s)$ of the shaking table to recognize the frequency range that the two curves match with each other mostly. If f_c is smaller than the lowest frequency of the frequency range, than only the displacement feedforward controller is adopted, i.e., W_a = 0 and W_x = 1. Similarly, W_a = 1 and W_x = 0 if f_c is greater than the largest frequency of the frequency range. Otherwise, the weighting W_a can be determined by applying interpolation method and W_x can be obtained by letting W_x = 1- W_a. The weighting interpolation method is illustrated in Fig. 3.

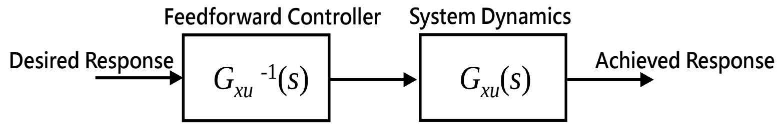

Fig. 1 –Illustration of the feedforward controller

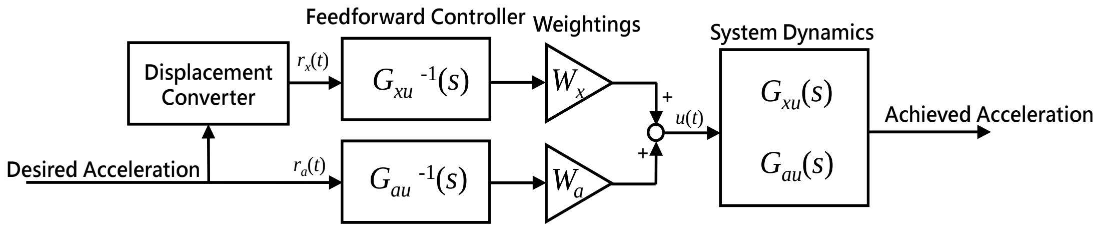

Fig. 2 –Block diagram of the proposed weighted feedforward controller implementation

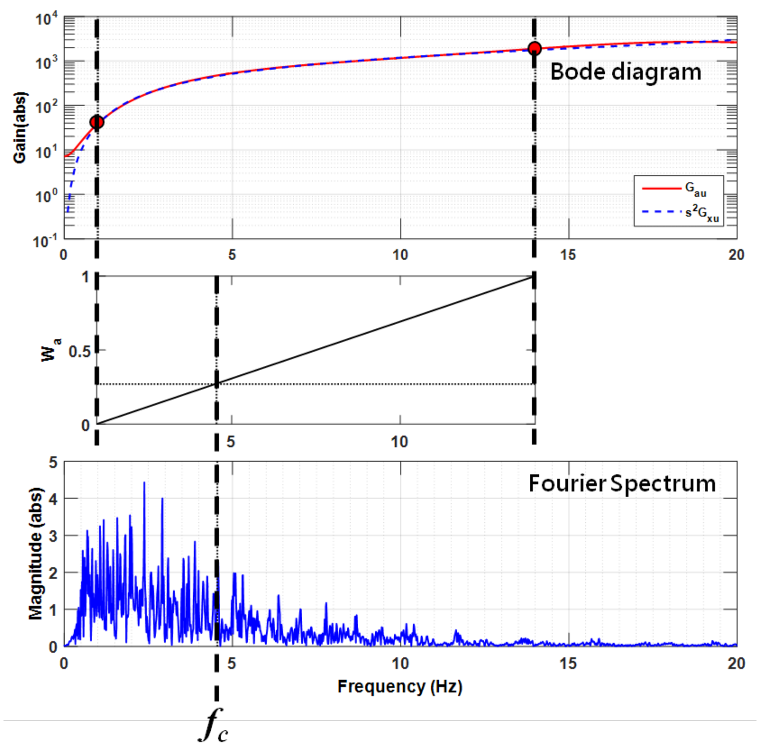

Fig. 3 –Illustration of the weighting interpolation method

3. Feedback Controller

In order to increase the robustness against the system uncertainty for shaking table control, a feedback controller designed by employing loop-shaping method is introduced. The design procedure proposed by Duncan McFarlane [8] is adopted to design the feedback controller incorporating the simple performance/robustness tradeoff obtained in loop shaping. The design technique has two main stages. First, loop shaping is used to shape the nominal plant singular values to give desired open-loop properties. Then, the normalized coprime factor H∞ problem is used to robustly stabilize this shaped plant. The design procedure is described below:

(1) Loop-Shaping: A pre-compensator $W_1(s)$, and/or a post-compensator $W_2(s)$ are used to shape the singular values of the nominal plant in order to have a desired open-loop shape. The nominal plant $G(s)$ and shaping functions W_1, W_2 are combined to form the shaped plant, $G_s(s)$, where $G_s(s)= W_2(s)\, G(s)\, W_1(s)$.

(2) Robust Stabilization: The maximum stability margin $b_{\max}$ is defined as

$$b_{\max}(G_s, K) \stackrel{\triangle}{=} \inf_{K\ stabilizing} \left\| \begin{bmatrix} K \\ I \end{bmatrix} (1 - G_s K)^{-1} \begin{bmatrix} I & G_s \end{bmatrix} \right\|_\infty^{-1} \tag{4}$$

where $G_s=M_s^{-1}N_s$, M_s and N_s are called normalized left coprime factorization of G_s. If $b_{\max}$ <<1 , then return to loop-shaping and modify $W_1(s)$ and $W_2(s)$. Finally, an $\varepsilon \leqq b_{\max}$ can be selected to synthesize a stabilizing controller $K\infty$, which satisfies

$$\left\| \begin{bmatrix} K_\infty \\ I \end{bmatrix} (1 - G_s K_\infty)^{-1} \begin{bmatrix} I & G_s \end{bmatrix} \right\|_\infty^{-1} \geq \varepsilon \tag{5}$$

Generally, $b_{\max} \geqq 0.3$ is claimed robust.

(3) The final feedback controller $K(s)$ is then constructed by combing the H∞ controller, $K\infty$, with the shaping functions $W_1(s)$ and $W_2(s)$ such that $K= W_1\, K\infty W_2$.

Figure 4 shows the design procedure of the loop-shaping design method. It is noted that the implementation of the feedback controller is not for improving the tracking performance, but for increasing the robustness of the shaking table test system. In addition, there is a tradeoff between system performance and robustness by using a feedback controller. Figure 5 depicts the controller framework for uni-axial shaking tables proposed in this study in which the feedforward controller aims to improve the acceleration tracking performance and the feedback controller intends to increase the system robustness against the uncertainty.

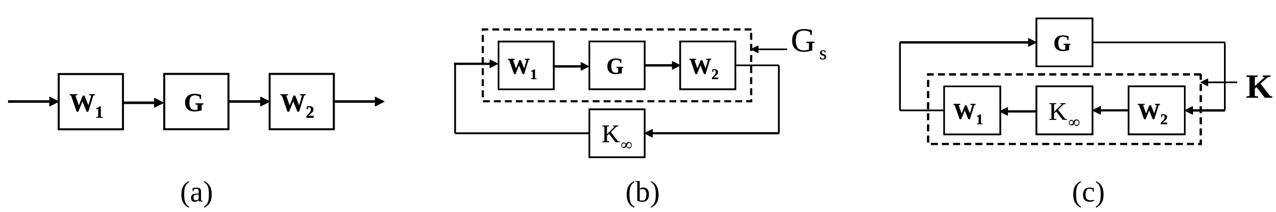

Fig. 4-Loop shaping design procedure (a) loop-shaping (b) robust stabilization (c) controller design

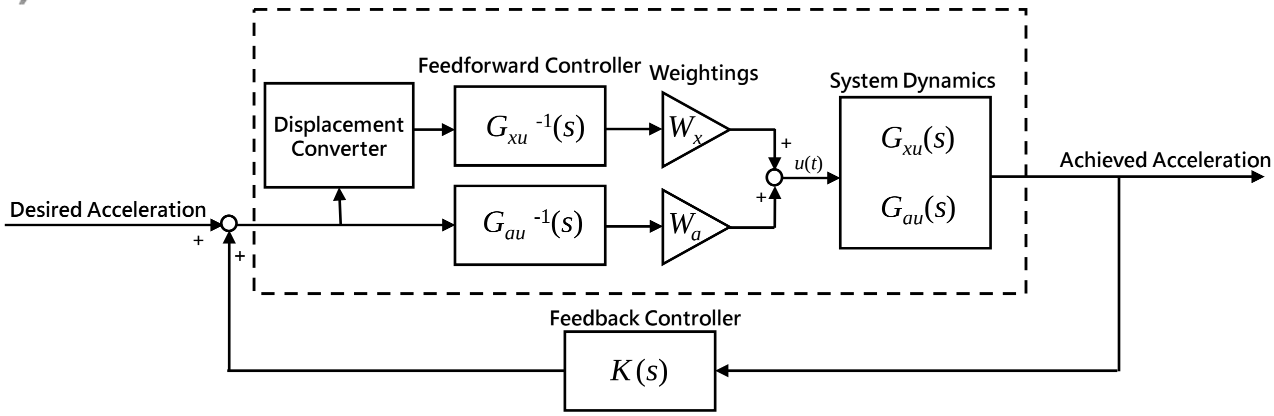

Fig. 5- The proposed control framework for uni-axial shaking tables

4. Experimental Setup and Controller Design

A two-story steel specimen is designed and assembled to evaluate the effectiveness of the proposed control framework implemented on a uniaxial shaking table at the National Center for Research on Earthquake Engineering (NCREE) in Taiwan. The uniaxial shaking table can be operated by using a portable test controller manufactured by Moog Inc. with well-tuned proportional and integral (PI) gains. A domestically assembled servo-hydraulic actuator is used to drive a 2500 mm x 1200 mm rigid platen made of aluminum. The maximum stroke and force capacity of the actuator are ±250 mm and ±100 kN, respectively. A couple of two-stage servo valves supplied by Star Hydraulic Ltd. are installed in parallel, providing a maximum flow rate up to 120 gallons per minute. Four hydrostatic bearings are used for the sliding mechanism in order to reduce the friction force while the table is moving. The allowable payload of the shaking table is limited to 10 kN due to the pull-resistant capacity of each hydrostatic bearing.

In the validation, dSPACE is adopted for implementing the outer-loop controllers as it is directly interfaced with MATLAB/Simulink running on a host computer. The DS1103 controller board, which is a system with real-time processor, provides fast input and output transmission for applications. By using Real-Time Interface (RTI), the outer-loop controller can be fully designed and analyzed in the environment employing Simulink functions and libraries. All the input and output can be configured as Simulink blocks by using RTI. The Simulink-based controller can be converted to real-time C code, compiled and downloaded to the DS1103 controller board. This real-time system collects the feedback signals from the shaking table and the references to compute the current command to the inner-loop control system. One linear variable differential transformer (LVDT) is embedded in the servo-hydraulic actuator to measure the table displacement which has been calibrated by a standard laser displacement sensor. In addition, one servo accelerometer named AS-2000, made by Tokyo Sokushin Cooperation Ltd., is installed on the shaking table to measure the table acceleration for the feedback controller. The experimental setup is shown in Fig. 6.

First, system identification tests are conducted to identify the shaking table test system. Transfer functions $G_{xu}(s)$ and $G_{au}(s)$ are identified which contain the dynamics of the servo-valve, actuator, PI controller, steel specimen, and measuring instruments. BLWN is adopted as the input command displacement with a range from 0 to 50Hz and a root mean square (RMS) power of 0.25 mm. The dSPACE DS1103 is used to generate the BLWN signal and measure the responses measured from the LVDT and the accelerometer with a sampling rate of 2000 Hz. The transfer functions are calculated with 512 FFT points, a Hanning window with 50% overlap, and 60 averages. Least square method is adopted to fit the experimental transfer function data for a single-input single-output model with selected numbers of poles and zeros. Eight system identification tests are conducted on various dates within six months to realize the system uncertainty of the shaking table. The corresponding system dynamics with the two-story specimen are shown in Fig. 7. The left part is the transfer function of the displacement white-noise excitation and the measured displacement. The right part is the transfer function of the identical input and the measured table acceleration. Dash lines in the figures indicate the first and second modes of the specimen. In the study, four poles and three zeros are selected for both the displacement and acceleration feedforward controllers $C_{xu}(s)$ and $C_{au}(s)$ which are given by

$$C_{xu}(s) = \frac{-1506s^3 + 3.074 \cdot 10^4 s^2 + 4.175 \cdot 10^6 s + 7.532 \cdot 10^7}{s^4 + 266.6s^3 + 3.07 \cdot 10^4 s^2 + 7.868 \cdot 10^5 s + 7.532 \cdot 10^7} \tag{6}$$

and

$$C_{au}(s) = \frac{0.3708s^3 + 64.35s^2 + 5673s + 8.808 \cdot 10^4}{s^4 + 136.1s^3 + 9275s^2 + 4.779 \cdot 10^4 s + 6.237 \cdot 10^4} \tag{7}$$

For feedback controller design, the selected pre-compensator $W_1(s)$ and post-compensator $W_2(s)$ should shape the plant to perform better at the low frequency range and reject the noise at the high frequency range. In this study, $W_1(s) = (s+0.5)/s^2$, and $W_2(s) = 1$ have been selected. The shaped loop-gain is shown in Fig. 8 with a gain cross-over frequency of 1.1 rad/sec. The stability margin $b_{\max}(G_s, K)$ is 0.3768 which satisfies the stability requirement. It is noted that the associated high-order controller may not be entirely necessary as its singular values are mostly governed by the largest three ones. Therefore, the MATLAB command "hankelmr" has been used to reduce the order of the controller. It has resulted in a reduced order model of K with information containing the error bound of the reduced model and Hankel singular values of the original system. The reduced 3rd-order controller is given by

$$K(s) = \frac{-2.897s^2 - 8.688s - 1.932}{s^3 + 9.497s^2} \tag{8}$$

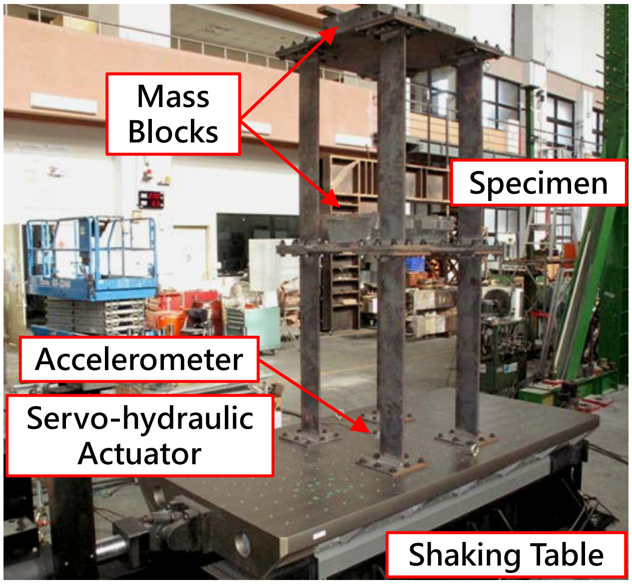

Fig. 6- Experimental setup

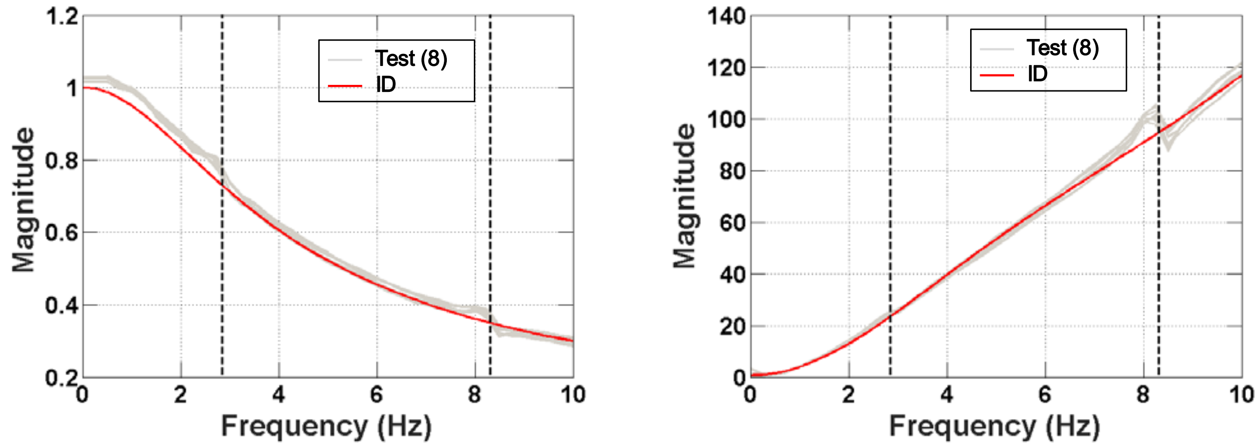

Fig. 7- System dynamics of shaking table identified on various dates

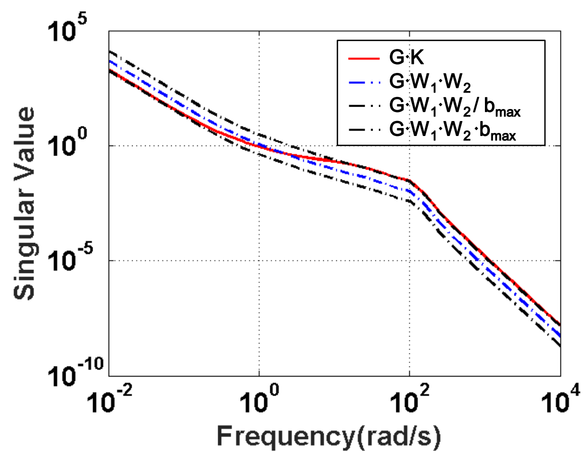

Fig. 8- Loop-shaping of the open-loop system

5. Experimental Results

Four acceleration time histories are adopted including two historical earthquake records and two artificial earthquakes. The 1940 El Centro and 1995 Kobe earthquakes are selected as they represent far-field and near-field ground motion records. GR-63-CORE and IEEE693 specifications [9] are adopted to generate the artificial earthquakes for experimental validation. The GR63-CORE provides test criteria for telecommunications equipment, switching and transport systems, associated cable distribution systems, distributing and interconnecting frames, power equipment, operations support systems, and cable entrance facilities [10]. IEEE standard requires that equipment and components of higher voltage classes must be seismically qualified by shaking table testing which is also frequently seen in seismic laboratories. The four acceleration time histories are normalized to a peak ground acceleration of 1 m/s^2 (100 gal). Five control schemes are applied to drive the shaking table: pure inner-loop PI control (denoted as PI), PI with additional outer-loop displacement feedforward control (denoted as DispFF + PI), PI with additional outer-loop acceleration feedforward control (denoted as AccelFF + PI), PI with additional outer-loop weighted feedforward control (denoted as WeightedFF + PI), and PI with additional outer-loop weighted feedforward control and feedback control (denoted as WeightedFF + FB +PI).

Two methods are adopted to evaluate the control performance of each ground motion reproduction in this study. First, the tracking performance of the shaking table control is investigated by using the RMS error in time domain which can be defined as

$$\mathrm{RMS_T}(\%) = \sqrt{\frac{\sum_{k=1}^{N}\left(a_r[k]-a_m[k]\right)^2}{\sum_{k=1}^{N}a_r[k]^2}} \times 100\% \tag{9}$$

where $a_r[k]$ and $a_m[k]$ are the reference and measured accelerations at the step k, respectively and N represents the number of the data points. Less difference between the reference and measured accelerations leads to a smaller RMS error; therefore, a low RMS error indicates good tracking performance. RMS error is also a normalized index since the square of error is divided by the square of reference, indicating that RMS error is not affected by the intensity of ground motion. The purpose of a shaking table test is to reproduce a predetermined acceleration time history; therefore, time lag and delay between the reference and measured accelerations is not critical. The tested specimen is subjected to an identical ground motion even though time lag and delay exists between the reference and measured accelerations. Consequently, time-shift correction must be completed before RMS error can be used as an index for evaluating the shaking table performance.

Meanwhile, Fourier magnitude spectrum is used to verify the frequency content of each ground motion in frequency domain. Therefore, the acceleration tracking of shaking table can be further investigated by using the RMS error of Fourier magnitude spectrum which can be defined as

$$\mathrm{RMS_F}(\%) = \sqrt{\frac{\sum_{k=1}^{N_F}\left(S_d[k]-S_a[k]\right)^2}{\sum_{k=1}^{N_F}S_d[k]^2}} \times 100\% \tag{10}$$

where $S_d[k]$ and $S_a[k]$ are the Fourier magnitude of the desired and achieved accelerations at the k-th frequency, respectively, and N_F represents the number of frequencies in Fourier Transform which should cover the frequency of interest. In the study, 0 to 20 Hz is adopted in the analysis.

Table 1 shows the RMS error on both time and frequency domain analyses. Evidently, the RMS errors in time and frequency domain are significantly reduced after applying the outer-loop controller regardless of the controller forms. In terms of the feedfoward controllers, the displacement feedforward controller performs slightly better than the acceleration feedforward controller in all the tests. In addition, the RMS errors in time and frequency domain are further reduced after combing both displacement and acceleration feedforward controllers. It indicates that the proposed weighted feedforward controller implementation has yielded improvement beyond either displacement or acceleration feedforward controller alone. On the other hand, the feedback controller designed by using loop-shaping method is not able to further improve the tracking performance comparing with the weighted feedforward controller scheme. It is considered reasonable since the feedback controller aims to enhance the system robustness which can be depicted in the loop-shaping result as shown in Fig. 8. It is noted that the high gain in the low frequency range contributes to the system performance while the low gain in the high frequency increases the system robustness. Since the design cutoff frequency is 1.1 rad/sec which implies the feedback controller design is mostly focused on the system robustness. The design cutoff frequency can be increased by applying different pre and post compensators $W_1(s)$ and $W_2(s)$. However, it would result in a smaller stability margin $b_{\max}$, leading to a difficulty to strengthen the system robustness through the implementation of the feedback controller. There is always a tradeoff between system performance and robustness by using a feedback controller.

The dynamics of the specimen would vary during a shaking table test due to the material and structural nonlinearity which could affect the tracking accuracy and even result in a stability issue of shaking table control. In this study, the robustness of the proposed control framework is estimated assuming the two-story steel specimen is completely demolished during the shaking table test by removing the specimen off the table.

Identical parameters of both feedforward and feedback controllers are used before and after the specimen is removed. Only the two historical earthquake records, the 1940 El Centro and 1995 Kobe, are selected as the acceleration reference. Table 2 shows the RMS errors in time and frequency domain of the test before and after the specimen is removed. It is found that the PI controller performs better for the tests when the specimen is removed. This is because the P and I gains are tuned for bare table for the sake of safety. Meanwhile, the feedback controller does improve the shaking table performance against system uncertainties compared with the feedforward and the PI controllers even though the improvement is not significant. On the other hand, the tracking performance of the displacement or acceleration feedforward controller becomes slightly inferior due to the change of system dynamics. However, the performance almost remains identical for the case with feedback controller regardless of the existence of the specimen. Conclusively, the test results demonstrate that the feedback controller improves the control robustness against the system uncertainty.

Table 1 –RMS error of time and frequency domain for tracking performance evaluation

Earthquake (m/s^2)	Controller	RMS_T(%)	RMS_F(%)
El Centro (1.0)	PI	35.47	28.25
	DispFF + PI	28.33	16.02
	AccelFF + PI	30.92	16.88
	WeightedFF + PI	27.96	16.01
	WeightedFF + FB + PI	28.12	16.47
Kobe (1.0)	PI	37.95	30.54
	DispFF + PI	23.99	15.96
	AccelFF + PI	24.90	16.69
	WeightedFF + PI	24.28	15.95
	WeightedFF + FB + PI	24.82	16.31
IEEE693 (1.0)	PI	48.75	41.08
	DispFF + PI	18.33	10.79
	AccelFF + PI	22.09	11.62
	WeightedFF + PI	16.59	10.34
	WeightedFF + FB + PI	19.31	10.86
GR63-CORE (1.0)	PI	34.54	28.92
	DispFF + PI	20.78	12.92
	AccelFF + PI	23.99	13.02
	WeightedFF + PI	20.33	11.85
	WeightedFF + FB + PI	20.68	12.15

Table 2 –RMS error of the time and frequency domain for system robustness evaluation

Earthquake (m/s^2)	Controller	Specimen on		Specimen off	
		RMS_T(%)	RMS_F(%)	RMS_T(%)	RMS_F(%)
El Centro (1.0)	PI	35.47	28.25	33.45	26.11
	DispFF + PI	28.33	16.02	30.96	17.74
	AccelFF + PI	30.92	16.88	31.15	18.03
	WeightedFF + PI	27.96	16.01	29.52	17.66
	WeightedFF + FB + PI	28.12	16.47	28.15	16.55
Kobe (1.0)	PI	37.95	30.54	35.57	28.12
	DispFF + PI	23.99	15.96	26.30	18.14
	AccelFF + PI	24.90	16.69	27.73	18.96
	WeightedFF + PI	24.28	15.95	26.89	18.85
	WeightedFF + FB + PI	24.82	16.31	25.15	16.77

6. Conclusions

A control framework for uniaxial shaking table control considering system performance and robustness has been proposed. The control framework incorporates feedforward and feedback control in which the feedforward controller improves the tracking performance while the feedback controller enhances the system robustness. Based on the frequency analysis of the acceleration time history to be reproduced, the weightings for displacement and acceleration feedforward controllers can be determined. The weighted feedforward control further improves the tracking performance compared with the system which is only applied the displacement or acceleration feedforward controller. In addition, the feedback controller improves the robustness against system uncertainty which has been proved by conducting the tests with and without the specimen on the table. The proposed control scheme guarantees that the shaking table test can be conducted with excellent tracking accuracy as well as strong system robustness.

7. References

[1] Spencer Jr. BF, Yang G (1998): Earthquake simulator control by transfer function iteration. *12th Engineering Mechanics Conference*, LaJolla, CA.

[2] Stoten DP, G'omez EG (2001): Adaptive control of shaking tables using the minimal control synthesis algorithm. *Philosophical Transactions of The Royal Society of London. Series A*: 1697-1723.

[3] Nakata N (2010): Acceleration trajectory tracking control for earthquake simulators. *Engineering Structures*, **32**(8), 2229-2236.

[4] Phillips BM, Wierschem NE, Spencer Jr. BF (2014): Model-based multi-metric control of uniaxial shake tables. *Earthquake Engineering & Structural Dynamics*, **43** (5), 681-699.

[5] Phillips BM, Spencer Jr. BF (2012): Model-based framework for real-time dynamic structural performance evaluation. *Newmark Structural Engineering Laboratory Report Series*, University of Illinois at Urbana-Champaign, Urbana, IL, No. 31.

[6] Asai T, Chang CM, Spencer Jr. BF (2014): Real-time hybrid simulation of a smart base-isolated building. *Journal of Engineering Mechanics*, **141**(3), 04014128.

[7] Dyke SJ, Spencer Jr. BF, Quast P, Sain MK (1995): Role of control-structure interaction in protective system design. *Journal of Engineering Mechanics*, **121**(2): 322-338.

[8] McFarlane D, Keith G (1992): A loop shaping design procedure using H_∞ synthesis. *IEEE Transactions on Automatic Control*, **37**(6), 759-769.

[9] IEEE Std 693TM-2005 (2006): IEEE recommended practice for seismic design of substations .*IEEE Power Engineering Society*, New York, USA.

[10] GR-63-CORE (2006):Network equipment building system (NEBS) requirements. Physical Protection, Issue 3.